

about ± 0.05 mK at the solid ordering. Using dP/dT from the curves of Fig. 3, the $\Delta Q/\Delta V$ data, and the liquid entropy, the solid entropy was obtained (not shown). From these curves, ordering temperatures of 1.9 and 2.15 mK are indicated for the 2.0- and 2.8-T fields, respectively. points follow the trend established by KMA (Ref. 2) for fields between 0.4 and 1.2 T. Unfortunately, the hysteresis and long time constants near the transition temperature do not permit reliable conclusions on the behavior of the entropy in this region. Furthermore, the above estimate of the latent heat in the transition indicates only a very small change in entropy.

Following the analysis of Adams, Delrieu, and Landesman,⁴ the magnetic susceptibility can be found from the relation

$$\chi_{B_1, B_2} = \left(\frac{2\Delta v}{v} \right) \frac{P_m(B_1) - P_m(B_2)}{B_2^2 - B_1^2}. \quad (3)$$

Here v is the molar volume of the solid at melting and Δv is the difference in molar volume between the liquid and solid. Using $B_1 = 2.0$ T and $B_2 = 2.8$ T, we find $\chi = 6.3 \times 10^{-6}$ and 5.5×10^{-6} at $T = 2.1$ and 2.6 mK, respectively. These values are in good agreement with those obtained in Ref. 4 from the data of Ref. 2 for lower fields.

In this work, the chart traces of pressure versus time have given evidence of a second phase transition in the solid in high fields. However,

further work is required for an understanding of the magnetic phases of solid ^3He . To aid in determining the type of spin ordering involved, we are preparing NMR experiments in conjunction with further latent-heat measurements.

We acknowledge useful discussion with E. B. Flint and G. G. Ihas. One of us (D.M.B.) thanks W. P. Halperin for fruitful conversations concerning these results. This work was supported by the National Science Foundation and partly by the Deutsche Forschungsgemeinschaft.

^(a)On leave from Fachbereich Physik, Universität Regensburg, Regensburg, West Germany.

¹W. P. Halperin, C. N. Archie, F. B. Rasmussen, R. A. Buhrmann, and R. C. Richardson, Phys. Rev. Lett. **32**, 927 (1974), and **34**, 718 (1975).

²R. B. Kummer, R. M. Mueller, and E. D. Adams, J. Low Temp. Phys. **27**, 319 (1977).

³T. C. Prewitt and J. M. Goodkind, Phys. Rev. Lett. **39**, 1283 (1977).

⁴E. D. Adams, J. M. Delrieu, and A. Landesman, J. Phys. (Paris), Lett. **39**, L190 (1978).

⁵W. J. Gully, D. D. Osheroff, D. T. Lawson, R. C. Richardson, and D. M. Lee, Phys. Rev. A **8**, 1633 (1973).

⁶D. D. Osheroff and P. W. Anderson, Phys. Rev. Lett. **33**, 686 (1974).

⁷D. D. Osheroff, thesis, Cornell University Report No. 1932, 1972 (unpublished).

Al Surface Relaxation Using Surface Extended X-Ray-Absorption Fine Structure

A. Bianconi

Istituto di Fisica, Università di Camerino, Camerino, Italy, and Stanford Synchrotron Radiation Laboratory, Stanford University, Stanford, California 94305

and

R. Z. Bachrach

Xerox Palo Alto Research Center, Palo Alto, California 94304

(Received 2 March 1978)

The surface extended x-ray-absorption fine structure (EXAFS) of a single crystal has been measured for the first time. By comparison with parameters obtained from bulk aluminum EXAFS, a decrease of the interatomic distance ($\Delta r = 0.15 \pm 0.05$ Å) at the Al(111) surface has been found. No relaxation is found of the Al-Al separation on the (100) face.

The difficulty of determining surface structure is one of the greatest barriers to the development of a better understanding of surface electronic states and bonding.¹ Low-energy electron diffraction (LEED)² is essentially the one estab-

lished technique for structure determination. This technique is limited to single-crystal analysis or chemisorbed atoms with a long-range order and has a low resolution. Recently by using synchrotron radiation as a source for x-ray spec-

troscopy, extended x-ray-absorption fine structure (EXAFS) has provided a new method for structure determination.^{3,4} In comparison with the LEED technique, EXAFS has a higher sensitivity to variations of the interatomic distance and can also be applied to amorphous surfaces. Lee has proposed the use of surface EXAFS measurements to determine adsorbate position.⁵

In this paper, we report the first surface EXAFS experiment performed on a clean single-crystal surface. We have studied the structural relaxation of the Al(111) and Al(100) surface. By using bulk aluminum EXAFS as a reference, a decrease of the interatomic distance $\Delta r = 0.15 \pm 0.05$ Å on the Al(111) surface has been found. No relaxation is found for the Al-Al distance on the Al(100) surface within the errors of the present experiment.

The experiment consists of measuring the quantum yield of secondary electrons originating from inelastically scattered L_{VV} Auger electrons generated in the decay of the absorption produced core hole. Using this partial yield technique, one measures the $L_{2,3}$ surface soft-x-ray absorption spectrum⁶ of a surface layer of thickness determined by the effective escape depth of the secondary or Auger electrons with the selected kinetic energy. The escape depth of electrons from aluminum in the energy range 35–65 eV can be on the order⁷ of 2 Å so that with the appropriate final-state energy, the $L_{2,3}$ absorption spectrum of approximately the first monolayer is measured. The sampling depth can be changed by using different final-state energies. The free-spectral range, however, is determined by the final-state energy plus the work function. Above this energy, direct photoemission is detected and part of the range is obscured. One should note that the secondary or Auger electrons detected at a fixed-state energy have a range different from the photogenerated electrons which result in the EXAFS. One should clearly differentiate the two separate processes.

The measurements reported were performed using the grazing-incidence monochromator⁸ on the 4° beam line at the Stanford Synchrotron Radiation Laboratory. The Al single crystal were cleaned by ion sputtering and annealing at 4×10^{-10} Torr. The residual oxygen contamination was less than 0.001 monolayer. The photoelectron energy was selected with a cylindrical mirror analyzer using a 3-eV energy window. The resolution of the spectra is determined by the monochromator and is on the order of 0.1 eV.

The linearly p -polarized light was incident near grazing ($\theta \leq 10^\circ$) and the electron analyzer detects a cone at $\theta = 42^\circ$. The direction of polarization used strongly emphasizes the interatomic distance normal to the surface.

Figure 1 shows the surface soft-x-ray absorption spectra of the Al(111) face measured collecting the inelastically scattered Auger electrons at 45 and 4 eV. At 45 eV final-state energy the surface sensitivity is close to maximum and only an average ~ 2.9 -Å layer [$2l^*(E) \cos \theta$] contributes to the spectrum. The surface layer of aluminum thus is the dominant contribution since the interatomic distance is 2.86 Å. For 4 eV final-state energy, the escape depth l^* is closer to 20 Å and the sampling volume is ~ 28 Å. Thus the 4-eV spectra should be dominated by the bulk contribution and the 45-eV spectra by the surface layer. The internal photoelectron energies are referenced to the L_3 edge at 72.72 ± 0.01 eV measured at the same energy in all the Al $2p$ spectra measured by us. By comparison with photoemission binding energy referenced to the Fermi energy, the largest final-state correction is 0.6 eV.⁹ The $E^* = 45$ eV spectrum has been taken up to 110 eV or just below the appearance of the Al $2p$ direct photoemission. The shift of the EXAFS structure toward higher energy in the $E^* = 45$ eV spectrum is clearly seen relative to the $E^* = 4$ eV curve showing directly that the surface interatomic dis-

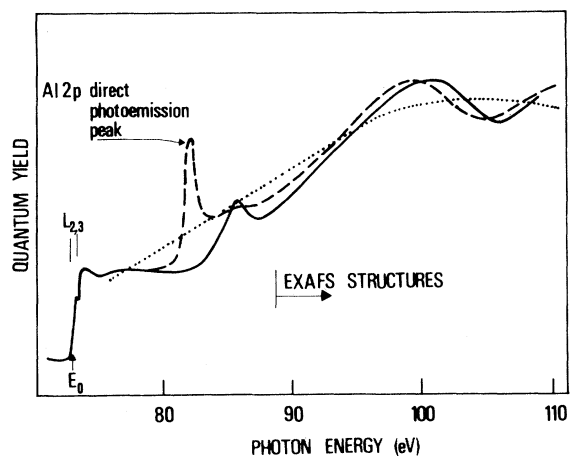


FIG. 1. Surface soft-x-ray absorption (SSXA) spectrum of the Al(111) surface. The solid line (SSXA) is obtained using the constant final-state energy $E^* = 45$ eV. The dashed line is obtained using $E^* = 4$ eV probing a much thicker layer and approximates the bulk absorption. The dotted line is the atomiclike Al $2p$ absorption cross section $\mu_0(\hbar\omega)$ used to extract the EXAFS modulations.

tance is shorter. The $E^* = 4$ eV spectral peak is, in fact, within 0.5 eV of that obtained from bulk aluminum EXAFS. In the remainder of the analysis, we will compare the $E^* = 45$ eV spectra with the bulk soft-x-ray absorption spectrum and use an approximation that the spectra is dominated by the outermost layer.

The $L_{2,3}$ soft-x-ray absorption spectra of simple metals such as aluminum is dominated by EXAFS oscillations.^{10, 11} The atomic calculation^{12, 13} of the absorption spectrum of the Al $2p$ electrons gives only a large broad peak as shown by the dotted curve in Fig. 1. The modulation of the cross section in the bulk Al spectrum results from EXAFS as has been previously conclusively established.^{10, 11} The smooth atomlike background absorption coefficient $\mu_0(\hbar\omega)$ is subtracted from the measured $\mu(\hbar\omega)$ absorption coefficient to obtain the modulation factor $\chi = (\mu - \mu_0)/\mu_0$ usually plotted in the EXAFS spectra.⁵

In Fig. 2 are shown the reduced χ EXAFS spectra of bulk Al, measured by optical transmission of an Al film and the surface EXAFS spectrum of Al(111) reduced from the original data shown in Fig. 1. Because the data are limited to a small energy range, only a fitting procedure could adequately extract the distance variations. We do this differentially with respect to parameters obtained for the bulk spectrum. The results should not depend strongly on the EXAFS approximation used to fit the data since variation of the distance between the same kinds of atoms is being measured.

The photoabsorption cross section for the $2p$

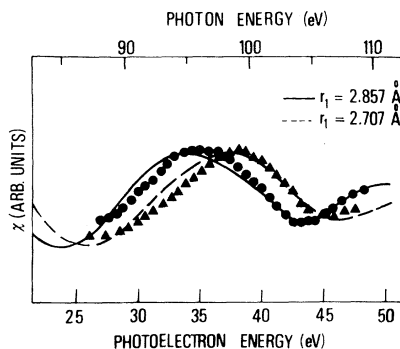


FIG. 2. Surface $L_{2,3}$ EXAFS spectrum of Al(111) surface (Δ curve) and bulk spectrum (solid-circle curve). $\chi(E) = (\mu - \mu_0)/\mu_0$ (where $E = \hbar\omega - E_0 + E_F$) is the modulation factor. The solid and dashed lines are the theoretical EXAFS spectra of bulk aluminum ($r_1 = 2.857$ Å) and of the Al(111) surface, respectively.

inner shell is given by

$$\sigma_{2p}(E) = \sigma_{2p}^0(E)[1 + \chi(E)],$$

where $E = \hbar\omega - E_0 + E_F$ is the photoelectron kinetic energy, E_0 is the energy of the $L_{2,3}$ edge, and E_F is the Fermi energy, 11.7 eV. In a free-electron-like metal, where $m^* \approx m_e$, the kinetic energy of the internally excited photoelectron is taken to be zero at the bottom of the conduction band. $\sigma_{2p}^0(E)$ is the broad atomlike absorption cross section and $\chi(E)$ is the modulation factor. $\chi(E)$ is determined by final-state interference effects through the transition matrix element. In spite of multiple scattering effects, it has been shown that the relatively simple theory gives satisfactory results for the $L_{2,3}$ spectra of simple metals.¹¹ Following Ref. 4 we have introduced the phase shift $\alpha_1(k)$ and following Ref. 5 the effect of the polarization of the radiation has been taken into account to calculate the surface EXAFS formula to fit the data so that

$$\chi(E) \propto \frac{-k}{2\pi} \sum_s A_s(k) \sum_j (\frac{1}{3} + \cos^2 \theta_{sj}) \exp(-2\gamma r_s) \times \text{Im}\{h_2(kr_s) \exp[i\alpha_2(k)]\}^2,$$

where h_2^+ is the spherical Hankel function of the first kind, $k = (0.263E)^{1/2}$, γ is the damping factor, and r_s is the distances of the neighboring atom shells. Only $2p$ - nd transitions are considered since they predominate in the L -shell absorption. $A_s(k)$ is the backscattering amplitude and $\alpha_2(k)$ is the phase shift experienced by the d -excited photoelectron. θ_{sj} is the angle between the x-ray polarization and the radial vector to the j th atom of the s th shell. When fitting the Al spectrum of bulk polycrystalline films, the sum over $\cos^2 \theta_{js}$ is replaced by N_s , the number of atoms in the s th shell. In the surface-EXAFS spectrum this factor eliminates the contribution of coplanar atoms when using grazing incidence p -polarized light because $\theta_{js} \approx \frac{1}{2}\pi$. Therefore the main contribution to the measured spectrum comes from the underlying atoms.

The fitting procedure was first applied to the bulk spectrum and good convergence was found with the bulk aluminum interatomic distance $r_1 = 2.857$ Å and $\lambda = 0.35$ Å⁻¹. $\alpha_2(k) = 0.05$ K has been used in agreement with the theoretical calculation of the $\alpha_2(k)$ phase shift for Al,¹⁴ in the $2.5 < k < 3.5$ Å⁻¹ range. In comparison with $\alpha_1(k)$, the value of $\alpha_2(k)$ is generally small and a monotonic function of k . Figure 2 shows the data point circles and the fit. Since the EXAFS modulations are being fit in a short energy range, both the k

dependence of the scattering factor and the energy dependence of the electron mean free path γ^{-1} should be small, but as expected the fitting is better at higher energies than at lower energies. The γ^{-1} value obtained from the fitting procedure is in good agreement with the average value of the escape depth of photoelectrons in the 15–35-eV energy range of initially excited photoelectrons.⁷

To fit the Al(111) surface EXAFS modulation, we have used the bulk determined damping factor and varied the r_1 distance and r_s by $\Delta r_s = \Delta d \cos \theta$; where Δd is the contraction of the spacing of the first two layers $d = 2.33 \text{ \AA}$ and θ is the angle between the surface normal and the direction toward the underlying atoms ($\Delta r_1 = \Delta d \cos 35^\circ$). By decreasing the distance r_1 , the maxima and minima of EXAFS shift towards higher energy and a good fit of the Al(111) surface EXAFS data is found with $\Delta r_1 = 0.15 \pm 0.05 \text{ \AA}$. This corresponds to a contraction of the first two layers spacing $\Delta d = 0.19 \pm 0.06 \text{ \AA}$. Figure 3 shows the Al(100) surface EXAFS spectrum and the calculated spectra with $\Delta r_1 = 0$ and $\Delta r_1 = 0.05 \text{ \AA}$. The estimated differential error on the extraction of interatomic distance is of the same order of magnitude 0.05 \AA . We can say that there is no relaxation of the Al(100) surface with a contraction of the interatomic distance greater than 0.05 \AA with respect to the bulk distance.

Our results can be compared with LEED intensity studies² of the Al(100) and Al(111) surface that have been reported. These experiments give no relaxation for the Al(100) surface in agreement with our result. The LEED results differ for the (111) face on the sign of the relaxation al-

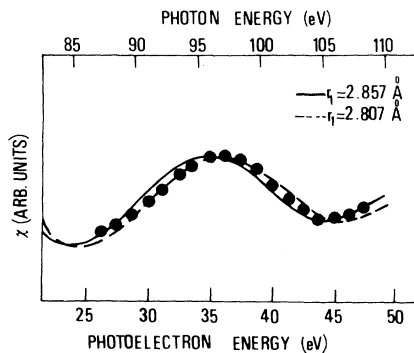


FIG. 3. Surface $I_{2,3}$ EXAFS spectrum of Al(100) surface (solid-circle curve). Solid and dashed lines are the theoretical spectrum using the bulk aluminum parameters and of a relaxed surface $\Delta r_1 = 0.05 \text{ \AA}$.

though the 5–10% magnitude range is the same. We observe that the EXAFS measurement directly give the relaxation as a contraction. The LEED technique has sensitivity with respect to variations of the spacing of the layers up to 0.1 \AA while the EXAFS is sensitive to variations of the interatomic distance as low^{3,4} as 0.01 \AA if many oscillations are measured.

In summary we have extracted structural information from the $L_{2,3}$ surface soft-x-ray absorption spectrum by fitting the first large EXAFS modulation. This work shows the possibility to measure a surface EXAFS spectrum of a clean surface and further work will be necessary to measure the spectrum on a larger energy range and to apply this technique to other materials. It is important to remark that this technique can also be applied to study amorphous surfaces.

The authors are grateful to the staff of the Stanford Synchrotron Radiation Laboratory for their support during the experiment. Thanks are due A. Balzarotti for supplying the computer program. We thank T. M. Hayes for helpful discussion. Some of the material incorporated in this work was developed with the financial support of the National Science Foundation (under Contract No. DMR7727489) in cooperation with the U. S. Department of Energy.

¹C. B. Duke, Mater. Sci. Eng. **25**, 13 (1976).

²M. R. Martin and G. A. Samorjai, Phys. Rev. B **7**, 3607 (1973); D. W. Jepsen, P. M. Marcus, and F. Jona, Phys. Rev. B **6**, 3684 (1972), and **5**, 3933 (1972).

³C. A. Ashley and S. Doniach, Phys. Rev. B **11**, 1279 (1975).

⁴T. M. Hayes, P. N. Sen, and S. H. Hunter, J. Phys. C **9**, 4357 (1976).

⁵P. A. Lee, Phys. Rev. B **13**, 5261 (1976).

⁶A. Bianconi, R. Z. Bachrach, and S. A. Flodstrom, Solid State Commun. **24**, 539 (1977), and references cited therein.

⁷C. J. Powell, R. J. Stein, P. B. Needham, Jr., and T. J. Driscoll, Phys. Rev. B **16**, 1370 (1977); R. Z. Bachrach, R. S. Bauer, J. C. McMenamin, and A. Bianconi, in Proceedings of the Fourteenth International Conference on the Physics of Semiconductors, Edinburgh, Scotland, September 1978 (to be published).

⁸F. C. Brown, R. Z. Bachrach, and N. Lien, Nuclear Instrum. Methods **152**, 103 (1978).

⁹J. J. Ritsko, S. E. Schnatterly, and P. C. Gibbons, Phys. Rev. Lett. **32**, 671 (1974).

¹⁰T. M. Hayes and P. N. Sen, Phys. Rev. Lett. **34**, 956 (1975).

¹¹H. Petersen and C. Kunz, Phys. Rev. Lett. **35**, 863

(1975); R. Haensel, G. Keitel, B. Sonntag, C. Kunz, and P. Schreiber, *Phys. Status Solidi (a)* **2**, 85 (1970).

¹²E. J. McGuire, *Phys. Rev.* **175**, 20 (1968).

¹³R. Z. Bachrach, D. J. Chadi, and A. Bianconi, to be published.

¹⁴G. D. Mahan, *Phys. Rev. B* **11**, 4814 (1975).

Onset of Ferromagnetism in $\text{Eu}_x\text{Sr}_{1-x}\text{S}$ near $x=0.5$

H. Maletta

Institut für Festkörperforschung der Kernforschungsanlage Jülich, 5170 Jülich, West Germany

and

P. Convert

Institut Laue-Langevin, 38042 Grenoble Cédex, France

(Received 8 September 1978)

In a neutron-diffraction study of insulating $\text{Eu}_x\text{Sr}_{1-x}\text{S}$ with $x=0.40, 0.50, 0.52$, and 0.54 , the critical concentration for the spin-glass-to-ferromagnetism transition is determined to be as high as $x_c=0.51$. For x just above x_c , magnetic microdomains coexist with long-range ferromagnetic order, decoupled from one another by competing antiferromagnetic bonds. For the first time the breakdown of ferromagnetic order into microdomains is directly observed by decreasing the temperature, and it is interpreted as a ferromagnetism-to-spin-glass transition.

The europium monochalcogenides are face-centered-cubic materials that are nearly ideal examples of the Heisenberg exchange model¹; for instance EuS orders ferromagnetically below $T_c=16.6$ K. There exists a model, theoretically studied by Kasuya,² that two kinds of exchange interactions, J_1 and J_2 , to the first and second nearest neighbors, respectively, with opposite sign are responsible for the ferromagnetic order in the insulator EuS. Recently³ the magnetic properties of EuS diluted with isostructural SrS have revealed a spin-glass-like behavior at low temperature in $\text{Eu}_x\text{Sr}_{1-x}\text{S}$ for $x \leq 0.5$, in spite of the samples not being metallic.

In this Letter we report on a neutron diffraction study of the spin-glass-to-ferromagnetism transition in $\text{Eu}_x\text{Sr}_{1-x}\text{S}$. Samples with $x=0.40, 0.50, 0.52$, and 0.54 were measured, and thereby the critical concentration for this transition is found to be at $x_c=0.51$. Combining the information supplied by the observed small-angle scattering and the scattering at the Bragg angles, the existence and behavior of microdomains⁴—defined as finite regions of magnetically ordered spins whose sizes are too small to be observed as sharp Bragg peaks—below and also above x_c are measured directly, as well as their influence on the onset of ferromagnetism.

Studies on the spin-glass-to-ferromagnetism transition in AuFe alloys have recently been published.⁵ Beside the metallurgical problem concerning clustering in such alloys, which is less

important in the solid-solution series of the isostructural insulators EuS and SrS,³ there may occur a change in character of the $3d$ states from "good" local moment to itinerancy just around the critical composition⁶; both features appear as complications for a model description. The magnetization and susceptibility measurements in small magnetic fields carried out in Ref. 5 give no direct evidence on the microscopic properties near x_c here under investigation. Earlier neutron-scattering experiments by Murani *et al.*⁷ on AuFe around x_c have only investigated the small-angle region.

The preparation of powdered samples of $\text{Eu}_x\text{Sr}_{1-x}\text{S}$ has been described in Ref. 3; they are enriched (99.1%) with ¹⁵³Eu as a result of the extremely high absorption cross section of ¹⁵¹Eu for thermal neutrons. The experiments have been performed at the D1B multicounter diffractometer of the Institut Laue-Langevin in Grenoble, using a wavelength of 2.52 Å.

In the neutron diffraction spectra of $\text{Eu}_x\text{Sr}_{1-x}\text{S}$ with $x=0.40$ and 0.50 , taken for scattering angles $4^\circ \leq 2\theta \leq 84^\circ$, no long-range magnetic order is observed down to the lowest accessible temperature of 1.6 K. In addition to the first three nuclear Bragg peaks, diffuse magnetic scattering intensity at small angles and around the Bragg angles is measured below 20 K, indicating short-range ferromagnetic order. These microdomains grow in size with decreasing temperature; the effect is more pronounced in the sample with higher Eu